JOURNAL OF AGRICULTURAL AND FOOD CHEMISTRY

J. Agric. Food Chem. **2007,** *55,* 5081–5091 **5081**

5-Hydroxy-3,6,7,8,3′,4′-hexamethoxyflavone Induces Apoptosis through Reactive Oxygen Species Production, Growth Arrest and DNA Damage-Inducible Gene 153 Expression, and Caspase Activation in Human Leukemia Cells

MIN-HSIUNG PAN,*,† YOU-SYUAN LAI,† CHING-SHU LAI,†,‡ YING-JAN WANG,‡ SHIMING LI,§ CHIH-YU LO,§ SLAVIK DUSHENKOV,|| AND CHI-TANG HO§

Department of Seafood Science, National Kaohsiung Marine University, Kaohsiung 811, Taiwan, Department of Environmental and Occupational Health, National Cheng Kung University Medical College, Tainan 704, Taiwan, Department of Food Science, Rutgers University, New Brunswick, New Jersey 08901, and WellGen, Inc., New Brunswick, New Jersey 08901

This study examined the growth inhibitory effects of structurally related polymethoxylated flavones in human cancer cells. Here, we report that 5-hydroxy-3,6,7,8,3′,4′-hexamethoxyflavone (5-OH-HxMF) induces growth inhibition of human cancer cells and induction of apoptosis in HL-60 cells through modulation of mitochondrial functions regulated by reactive oxygen species (ROS). ROS generation occurs in the early stages of 5-OH-HxMF-induced apoptosis, preceding cytochrome *c* release, caspase activation, and DNA fragmentation. The changes occurred after single breaks in DNA were detected, suggesting that 5-OH-HxMF induced irreparable DNA damage, which in turn triggered the process of apoptosis. Up-regulation of Bax was found in 5-OH-HxMF-treated HL-60 cells. In addition, a caspase-independent pathway indicated by endonuclease G also contributed to apoptosis caused by 5-OH-HxMF. Antioxidants suppress 5-OH-HxMF-induced apoptosis. 5-OH-HxMF markedly enhanced growth arrest DNA damage-inducible gene 153 (GADD153) protein in a time-dependent manner. *N*-acetylcysteine (NAC) and catalase prevented up-regulation of GADD153 expression caused by 5-OH-HxMF. These findings suggest that 5-OH-HxMF creates an oxidative cellular environment that induces DNA damage and GADD153 gene activation, which in turn helps trigger apoptosis in HL-60 cells. Meanwhile, ROS were proven an important inducer in this apoptotic process. The C-5 hydroxyl on the ring of 5-OH-HxMF was found to be essential for the antiproliferative and apoptosis-inducing activity. Our study identified the novel mechanisms of 5-OH-HxMF-induced apoptosis and indicated that these results have significant applications as potential chemopreventive and chemotherapeutic agents.

KEYWORDS: Polymethoxylated flavones; apoptosis; cytochrome *c*; caspase-9; caspase-3; poly-(ADP-ribose) polymerase; antioxidant; GADD153; reactive oxygen species

INTRODUCTION

Citrus flavonoids, especially polymethoxyflavones (PMFs), have a broad spectrum of biological activity including anticarcinogenic, anti-inflammatory, and antitumor activities (*1*, *2*). Because of the hydrophobic nature of methoxy groups relative to hydroxyl groups, PMFs, such as tangeretin and nobiletin, are more lipophilic and are better inhibitors of tumor cell growth than the hydroxylated flavonoids, such as rutin, quercetin, and myricetin (*3*). The PMFs may have higher permeability through the small intestine and are readily absorbed into the blood circulation system of the human body (*4*). PMFs exist almost exclusively in the citrus genus, particularly in the peel of sweet oranges (*Citrus sinensis*) and mandarin oranges (*Citrus reticulate*).

It is commonly recognized that cancer induction can be prevented by ingestion of certain foods, and flavonoids in *Citrus* fruits and juices are one of the most prominent cancer-preventing agents (*5*, *6*). A large number of chemopreventive and chemotherapeutic agents, from natural products, have been used as a promising strategy to fight against cancer by inducing apoptosis in malignant cells (*7*). Apoptosis is defined as a type of cell death, involving the concerted action of a number of intracellular signaling pathways, including members of the caspase family of cysteine proteases, stored in most cells as zymogens or

* To whom correspondence should be addressed. Tel: 886-7-361-7141 ext. 3623. Fax: 886-7-361-1261. E-mail: mhpan@mail.nkmu.edu.tw.
† National Kaohsiung Marine University.
‡ National Cheng Kung University Medical College.
§ Rutgers University.
|| WellGen, Inc.

10.1021/jf070068z CCC: $37.00
Published on Web 05/31/2007

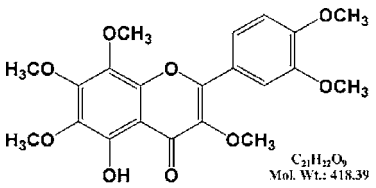

5- hydroxy- 3,6,7,8,3',4'-
hexamethoxyflavone (5-OH-HxMF)

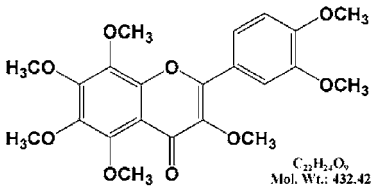

3,5,6,7,8,3',4'- hepamethoxyflavone (HpMF)

Figure 1. Chemical structures of ″5-OH-HxMF and ″HpMF.

procaspases (*8*). Proteolytic cleavage of procaspases is an important step leading to caspase activation, which in turn is amplified by the cleavage and activation of other downstream caspases in the apoptosis cascade (*8*). The two main apoptotic pathways, the death receptor (extrinsic) and mitochondrial (intrinsic) pathways, are activated by caspase-8 and caspase-9, respectively. Caspase-8 is recruited as a death-inducing signaling complex only when death receptors such as Fas or the tumor necrosis factor receptor bind to specific multimeric ligands. In contrast, caspase-9 is activated when cytochrome *c* is released into cytoplasm from the mitochondrial intermembranous space. Activated caspase-8 and caspase-9 activate executioner caspases, including caspase-3, which in turn cleave a number of cellular proteins that include structural proteins, nuclear proteins, cytoskeletal proteins, and signaling molecules (*9*). Moreover, the mitochondrial pathway is regulated by the Bcl-2 family of proteins, including antiapoptotic proteins such as Bcl-2 and Bcl-X_L and proapoptotic proteins such as Bad, Bid, Bim, Bax, and Bak (*9*). Recent studies of the endoplasmic reticulum (ER) as a third subcellular compartment containing caspases were implicated in apoptotic execution induced by ER stress (*10*, *11*). The ER stress-induced cell death modulator is a CCAAT/enhancer-binding protein (CEBP) homology protein (CHOP)/growth arrest and DNA damage-inducible gene 153 (GADD153), known as CHOP, and is a member of the CEBP family of transcription factors (*11*). Expressed at low levels in proliferating cells, it is strongly induced in response to stresses that result in growth arrest or cellular death, including oxidant injury, DNA damaging agents such as peroxynitrite, UV radiation, anticancer chemotherapy, and ER stress (*12*). Recent studies suggest that GADD153 plays a central role in the apoptosis induction by overexpression of GADD153 of vector-transfected cells, including the dephosphorylation of the proapoptotic protein Bad and down-regulation of Bcl-2 expression (*13*).

In this study, we selected 5-hydroxy-3,6,7,8,3′,4′-hexamethoxyflavone (5-OH-HxMF) and 3,5,6,7,8,3′,4′-heptamethoxylflavone (HpMF) (**Figure 1**) for evaluation of their anticancer properties in various human cancer cells. The only structural difference between 5-OH-HxMF and HpMF is on the 5-position of A ring: The methoxy group on the 5-position of A ring of the 5-OH-HxMF is demethylated to become the hydroxy group of the HpMF. It is interesting to note that, on the basis of our present studies, 5-OH-HxMF is far more potent than HpMF (less lipophilic) at inhibiting the proliferation and inducing apoptosis in HL-60 cells. However, to date, no information is available regarding the mechanism of the effects of 5-OH-HxMF on human leukemia HL-60 cells. To gain a better understanding of the molecular effects of 5-OH-HxMF on human leukemia cells, we focused on the primary aim of the cellular environment in HL-60 cells that can influence the expression of the GADD153 protein in causing cell death. This included studies on the effects of 5-OH-HxMF on the activation of reactive oxygen species (ROS) production and caspase cascade, expression of Bcl-2, Bcl-X_L, and Bax, and changes in expression of GADD153 gene in HL-60 cells.

MATERIALS AND METHODS

Cell Culture and Chemicals. Human promyelocytic leukemia (HL-60) cells obtained from American Type Culture Collection (Rockville, MD), COLO 205 cells, HT-29 cells, Jurkat cells, U937 cells, and THP-1 cells were grown in RPMI 1640 medium and 10% fetal bovine serum (Gibco BRL, Grand Island, NY) supplemented with 2 mM glutamine (Gibco BRL) and 1% penicillin/streptomycin (10000 units of penicillin/mL and 10 mg/mL streptomycin). Human polymorphonuclear cells (PMNs) were obtained from healthy male donors and were separated by a Ficoll−Hypaque density gradient. Human PMNs were washed twice in 0.9% NaCl and resuspended in RPMI-1640 medium. The human AGS gastric carcinoma cells (CCRC 60102) were obtained from the Food Industry Research and Development Institute (Hsinchu, Taiwan) and cultured in Dulbecco's modified Eagle's medium/nutrient mixture F-12 containing 10% heat-inactivated fetal bovine serum (Gibco BRL), 100 units/mL of penicillin, 100 μg/mL of streptomycin, and 2 mM L-glutamine (Gibco BRL) and kept at 37 °C in a humidified 5% CO_2 incubator. Pan-caspase inhibitor (z-Val-Ala-Asp-fluoromethyl ketone, z-VAD-FMK) was purchased from Calbiochem (La Jolla, CA). Propidium iodide was obtained from Sigma Chemical Co. (St. Louis, MO).

General Preparative High-Performance Liquid Chromatography (HPLC) Separation Procedures from Crude Sweet Orange Peel Extract (OPE, Cold-Pressed Oil). The commercial OPE mixture from Florida Flavors Co. (Lakeland, FL) (30 g) was dissolved in a mixture of methylene chloride (2 mL) and hexanes (2 mL) and loaded onto a 330 g preconditioned silica gel flash column. The gradient was started with 10% ethyl acetate and 90% hexanes and went to 40% ethyl acetate and 60% hexanes within 40 min. Then, the isocratic mobile phase (40% ethyl acetate−60% hexanes) was applied for another 15 min (total run of 55 min). The fractions that had UV absorbance at 254 nm were analyzed by liquid chromatography−electrospray ionization−mass spectrometry (LC-ESI-MS) and the fractions displaying parent peaks, MH^+ at 419 (″5-OH-HxMF) and MH^+ at 433 (″HpMF), were combined, concentrated, and further separated, respectively, using chiral separation procedures (see below).

Separation Procedures of Hydroxylated PMFs by Chiral HPLC. The two residues from the flash column containing ″5-OH-HxMF and ″HpMF (characterized by LC-ESI-MS) were dissolved in a minimal amount of methylene chloride, respectively. The solution was then loaded onto an HPLC system equipped with the Welk-O 1 (R,R) Regis column (450 g) separately for those two residues (Waters Delta Prep 4000 delivery pump, Milford, MA). The mobile phase was composed of 30% absolute alcohol and 70% hexanes, and the monitoring UV wavelength was set at 280 nm. Pure ″HpMF and ″5-OH-HxMF were eluted, and the fractions were collected and concentrated. MS, UV, and proton and ^{13}C NMR were used to identify pure compounds. Analytical HPLC conditions on HPLC-MS were as follows: column, Chromeabond WR C_{18}, 3 μm, 120; length and OD, 30 mm × 3.2 mm; injection volume, 15 μL; flow rate, 2 mL/min; and run time, 3 min. The mobile phase consisted of acetonitrile and H_2O with 0.05% trifluoroacetic acid, a typical gradient of 10−90% acetonitrile, and the gradient varied.

Cell Proliferation Assay. Cell viability was assayed by trypan blue exclusion assay. Briefly, human cancer cells were plated at a density of 1×10^5 cells/mL into 24 well plates. After overnight growth, cells were pretreated with a series of concentrations of 5-OH-HxMF and HpMF for 24 h. The final concentration of dimethyl sulfoxide (DMSO)

in the culture medium was <0.05%. At the end of treatment, the cells were harvested after 24 h. Viability was determined by trypan blue exclusion and microscopy examination.

DNA Extraction and Electrophoretic Analysis. The HL-60 human leukemia cells were harvested, washed with phosphate-buffered saline (PBS), and then lysed overnight at 56 °C with a digestion buffer containing 0.5% sarkosyl, 0.5 mg/mL proteinase K, 50 mM tris-(hydroxymethyl)aminomethane (pH 8.0), and 10 mM ethylenediaminetetraacetic acid (EDTA). Following these lyses, the cells were then treated with RNase A (0.5 μg/mL) for 3 h at 56 °C. The DNA was then extracted using phenol/chloroform/isoamyl isoamyl alcohol (25:24:1) prior to loading and was analyzed by 2% agarose gel electrophoresis. The agarose gels were run at 50 V (20 mA) for 120 min in Tris-borate/EDTA electrophoresis buffer. Approximately 20 μg of DNA was loaded into each well, DNA was stained with ethidium bromide and visualized under UV light (260 nm), and the plates were photographed (*14*).

Acridine Orange Staining Assay. Cells (5×10^5) were seeded into 60 mm Petri dishes and incubated at 37 °C for 24 h. The cells were harvested, and 5 μL of suspended cells was mixed on a slide with an equal volume of acridine orange solution (10 μg/mL in PBS). Green fluorescence was detected between 500 and 525 nm by using an Olympus microscope (CK40, Olympus America, Inc., Lake Success, NY). Apoptotic cells were distinguished from viable cells by showing homogeneously bright staining in nuclei, however, with chromatin condensation indicative of apoptosis.

Flow Cytometry. HL-60 cells (2×10^5) were cultured in 60 mm Petri dishes and incubated for 24 h. The cells were then harvested, washed with PBS, resuspended in 200 μL of PBS, and fixed in 800 μL of iced 100% ethanol at −20 °C. After they were left to stand overnight, the cell pellets were collected by centrifugation, resuspended in 1 mL of hypotonic buffer (0.5% Triton X-100 in PBS and 0.5 μg/mL RNase), and incubated at 37 °C for 30 min. Next, 1 mL of propidium iodide solution (50 μg/mL) was added, and the mixture was allowed to stand on crushed water ice for 30 min. Fluorescence emitted from the propidium iodide−DNA complex was quantitated after excitation of the fluorescent dye by FACScan cytometry (Becton Dickinson, San Jose, CA). Quantitation of the fraction of each cell cycle stage was performed with ModFit LT for Mac 3.0 software (Becton Dickinson).

ROS Production Determination. Cells were treated with 5-OH-HxMF (100 μM) for different time periods, and dichlorodihydrofluorescein diacetate (DCFH-DA; 20 μM) or DHE (20 μM) was added to the medium for a further 30 min at 37 °C. ROS production was monitored by flow cytometry using DCFH-DA. This dye is a stable, nonpolar compound that readily diffuses into cells and is hydrolyzed by intracellular esterase to yield DCFH, which is trapped within the cells. Hydrogen peroxide or low molecular weight peroxides produced by the cells oxidize DCFH to the highly fluorescent compound 2′,7′-dichlorofluorescein (DCF). Thus, the fluorescence intensity was proportional to the amount of peroxide produced by the cells.

Analysis of Mitochondrial Trans-Membrane Potential. The change of the mitochondrial trans-membrane potential was monitored by flow cytometry. Briefly, HL-60 cells were exposed to 5-OH-HxMF (100 μM) for different time periods, and the mitochondrial trans-membrane potential was measured directly using 40 nM 3,3′-dihexyloxacarbocyanine [DiOC6(3)] (Molecular Probes, Eugene, OR). Fluorescence was measured after staining the cells for 30 min at 37 °C. The mitochondrial membrane potential was quantitated by the flow cytometric analysis of DiOC6(3)-stained cells. Lipophilic cation, such as the fluorescent dyes DiOC6(3), was transported into the mitochondria by the negative mitochondrial membrane potential and thus concentrated within the mitochondrial matrix. Histograms were analyzed using Cell Quest software and were compared with histograms of untreated, control cells.

Preparation of Subcellular Fraction. Subcellular fraction was performed as described previously (*15*). Briefly, cells were trypsinized and washed once with ice-cold PBS following lysing in lysis buffer [250 mM scrose, 1 mM EDTA, 0.05% digitonin, 25 mM Tris (pH 6.8), 1 mM dithiothreitol, 10 μg/mL pepstatin, 10 μg/mL aprotinin, 1 mM benzamidine, and 0.1 mM phenylmethylsulfonyl fluoride (PMSF)] and were homogenized (20 strokes with a B-pestle Dounce homogenizer). The lysate was centrifuged (750*g* for 5 min) to remove nuclei and unlysed cells and centrifuged again (10000*g* for 10 min) to obtain the mitochondria fraction (pellet). The supernatant was centrifuged at 14000*g* for 1 h to obtain the cytosolic fraction. The mitochondria fraction was solubilized in gold lysis buffer containing 50 mM Tris-HCl (pH 7.4), 1 mM NaF, 150 mM NaCl, 1 mM EGTA, 1 mM phenylmethanesulfonyl fluoride, 1% NP-40, and 10 μg/mL leupeptin.

Western Blotting. For the determination of the expression of Bcl-2 family, cytochrome *c*, AIF, and Endo G protein, the nuclear and cytosolic proteins were isolated from HL-60 cells after treatment with 25 μM 5-OH-HxMF for 0, 3, 6, 9, 12, and 24 h. The total proteins were extracted via the addition of 200 μL of gold lysis buffer [50 mM Tris-HCl (pH 7.4), 1 mM NaF, 150 mM NaCl, 1 mM EGTA, 1 mM phenylmethanesulfonyl fluoride, 1% NP-40, and 10 μg/mL leupeptin] to the cell pellets on ice for 30 min, followed by centrifugation at 10000*g* for 30 min at 4 °C. The cytosolic fraction (supernatant) proteins were measured by the Bio-Rad protein assay (CA 94547, Bio-Rad Laboratories, Hercules, Munich, Germany). The samples (50 μg of protein) were mixed with five-fold sample buffer containing 0.3 M Tris-HCl (pH 6.8), 25% 2-mercaptoethanol, 12% sodium dodecyl sulfate (SDS), 25 mM EDTA, 20% glycerol, and 0.1% bromophenol blue. The mixtures were boiled at 100 °C for 5 min and were prerun on a stacking gel and then resolved by 12% SDS-polyacrylamide minigels at a constant current of 20 mA. Subsequently, electrophoreses were carried out on SDS-polyacrylamide gels. For electrophoresis, proteins on the gel were electrotransferred onto a 45 μm immobile membrane (PVDF; Millipore Corp., Bedford, MA) with transfer buffer composed of 25 mM Tris-HCl (pH 8.9), 192 mM glycine, and 20% methanol. The membranes were then blocked with blocking solution [20 mM Tris-HCl (pH 7.4), 0.2% Tween 20, 1% bovine serum albumin, and 0.1% sodium azide]. The membrane was further incubated with the respective specific antibodies, at the appropriate dilution (1:1000) using various blocking solution, such as anti-Bcl-2, anti-Bcl-X_L, anti-Bax, anti-GADD153, anti-β-actin (Santa Cruz Biotechnology), anti-PARP [poly(ADP-ribose)polymerase] (UBI, Inc., Lake Placid, NY), anti-Bid, anti-AIF, anti-Endo G (Transduction Laboratory, Lexington, KY), and anti-DNA fragmentation factor (DFF)-45/inhibitor of caspase-activated DNase (ICAD) antibody (MBL, Naka-Ku, Nagoya, Japan) at room temperature for 1 h. The membranes were subsequently probed with anti-mouse or anti-rabbit IgG antibody conjugated with horseradish peroxidase (Transduction Laboratories, Lexington, KY), and detection was achieved by measuring the chemiluminescence of the blotting agents (ECL, Amersham Corp., Arlington Heights, IL), by exposure of the filters to Kodak X-Omat films. The densities of the bands were quantitated with a computerized densitometer system (AlphaImager 2200 System, Alpha Innotech Corp., San Leandro, CA). The mitochondrial and cytosolic fractions isolated from the cells were used for immunoblot analysis of cytochrome *c* as previously described (*16*). The cytochrome *c* protein was detected using an anti-cytochrome *c* antibody (Research Diagnostic Inc., Flanders, NJ).

Activity of Caspase. Cells were collected and washed with PBS and suspended in 25 mM HEPES (pH 7.5), 5 mM $MgCl_2$, 5 mM EDTA, 5 mM dithiothione, 2 mM phenylmethanesulfonyl fluoride, 10 μg/mL pepstatin A, and 10 μg/mL leupeptin after treatment. Cell lysates were clarified by centrifugation at 12000*g* for 20 min at 4 °C. The caspase activity in the supernatant was determined by a fluorogenic assay (Promeaga's CaspACE Assay System Corp., Madison, WI). As described previously (*17*), briefly, 50 μg of total protein, as determined by the Bio-Rad protein assay kit (Bio-Rad Laboratories), was incubated with 50 μM substrate Ac-Try-Val-Ala-Asp-AMC (Ac-YVAD) (caspase-1 specific substrate), Ac-Val-Asp-Val-Ala-Asp-AMC (Ac-VDVAD-AMC) (caspase-2-specific substrate), Ac-Asp-Glu-Val-Asp-AMC (Ac-DEVD-AMC) (caspase-3 specific substrate), Ac-Ile-Glu-Thr-Asp-AMC (Ac-IETD-AMC) (caspase-8 specific substrate), or Ac-Leu-Glu-His-Asp-AMC (Ac-LEHD-AMC) (caspase-9 specific substrate) at 30 °C for 1 h. The release of methylcoumaryl-7-amine (AMC) was measured by excitation at 360 nm and emission at 460 nm using a fluorescence spectrophotometer (ECLIPSE, Varian, Palo Alto, CA).

Assessment of DNA Damage. The DNA damage level caused by 5-OH-HxMF was measured as previously described (*18*). HL-60 cells

Table 1. Effect of Different Compounds on the Growth of Various Human Cancer Cells[a]

cell line	compound IC_{50} (μM)	
	5-OH-HxMF	HpMF
AGS	17.01 ± 0.21	>100
COLO205	67.02 ± 1.40	62.5 ± 1.81
HT-29	77.38 ± 1.82	>100
HL-60	5.61 ± 0.07	>100
Jurkat	88.94 ± 0.71	>100
monocyte	>100	>100
THP-1	>100	>100
U937	78.42 ± 6.36	>100

[a] Cells were treated with various concentrations of selected compounds for 24 h. Cell viability then was determined by the trypan blue assay as described. Each experiment was independently performed three times and expressed as mean ± SD.

were pretreated with antioxidants for 2 h, prior to exposure to 5-OH-HxMF (25 μM); cells were then suspended in agarose gel, and the suspension was pipetted onto glass slides. Following treatment of the supported cells with alkaline detergent to remove cellular membranes, the resulting nucleoids were subjected to electrophoresis. Slides were then placed in a horizontal electrophoresis tank with freshly prepared cold electrophoresis buffer (0.3 M NaOH and 1 mM EDTA, pH > 13) for 30 min at 4 °C and submitted to electrophoresis (20 V) for 15 min. The DNA of the nucleoids was stained with ethidium bromide to permit visualization using a fluorescence microscope at 100×, with an exciting filter of 515−560 nm and a barrier filter of 590 nm (same Olympus).

Statistical Analysis. The statistical significance of differences between the means was evaluated using the Student's test. A difference with a p value less than 0.05 was considered statistically significant. All statistical analyses were carried out using the SAS package.

RESULTS

Inhibition of Cell Proliferation in 5-OH-HxMF-Treated Human Cancer Cells. The effects of 5-OH-HxMF and its analogues HpMF on cell growth were evaluated in various human cancer cells. The chemical structure of both compounds is shown in **Figure 1**. To assess the inhibitory effects of these compounds on the growth of human cancer cells, the cells were cultured for 24 h with or without test compound (5−100 μM), and the cell growth rate was determined by trypan blue assay. As shown in **Table 1**, the antiproliferation activity of 5-OH-HxMF was observed in cancer cell lines but not in primary human PMNs and THP-1 cells (IC_{50} > 100 μM). 5-OH-HxMF selectively inhibited cancer cell proliferation. This was demonstrated by decreased cell growth in the cultured human cancer cells. Cell growth was suppressed in AGS, COLO 205, HT-29, HL-60, Jurkat, and U937 in a dose-dependent manner, with IC_{50} values of 17.01, 67.02, 77.38, 5.61, 89.44, and 78.42 μM, respectively. Overall, the antiproliferative activity of 5-OH-HxMF in human cancer cell lines was much more pronounced as compared to HpMF. Only in COLO 205 cells was the antiproliferation activity of HpMF comparable to 5-OH-HxMF. The antiproliferative effect of 5-OH-HxMF was most pronounced in HL-60 cells. This cell line was selected for further examination of 5-OH-HxMF's cytotoxic effects.

5-OH-HxMF Induces Apoptosis in Human Leukemia HL-60 Cells. Physiological cell death is characterized by apoptotic morphology, including chromatin condensation, membrance blebbing, internucleosome degradation of DNA, and apoptotic body formation. In each case, nucleosomal DNA ladders (*19*), which are indicative of apoptosis, are visible on agarose gel after staining with ethidium bromide. To evaluate the potential mechanism of the cytotoxic effects, HL-60 cells were treated with 5-OH-HxMF and HpMF for 24 h followed by DNA fragmentation analyses. As shown in **Figure 2A**, significant DNA ladders were observed in HL-60 cells treated with 5 μM 5-OH-HxMF for 24 h in contrast to no data, suggesting evidence of apoptotic induction by HpMF, even at concentrations of 25 μM. Evaluation of DNA fragmentation at 0, 3, 6, 9, 12, and 24 h revealed that after treatment with 25 μM 5-OH-HxMF, digested genomic DNA was already evident at 9 h (**Figure 2B**). Flow cytometry was used to investigate the induction of a sub-G1 cell population, a hallmark of apoptosis. HL-60 cells were treated with 5-OH-HxMF (0−25 μM) and stained with propidum iodide. As seen in **Figure 2C**,**D**, the percentages of apoptotic HL-60 cells were 2.85, 14.9, 47.10, and 64.11%, respectively, after incubation with 0, 5, 10, and 25 μM for 24 h, and 7.03, 9.55, 17.16, 30.46, 38.44, and 68.41% after 0, 3, 6, 9, 12, and 24 h of incubation with 5-OH-HxMF (25 μM), respectively. A rapid increase in the number of apoptotic HL-60 cells at 9 h after treatment with 25 μM 5-OH-HxMF is well-correlated with visible DNA laddering effects.

The cell death induced by 5-OH-HxMF was characterized by examining the nuclear morphology of dying cells using a fluorescent DNA-binding agent, acridine orange. Within 24 h of treatment with 25 μM 5-OH-HxMF, cells clearly exhibited significant morphological changes and chromosomal condensation, indicative of apoptotic cell death (**Figure 2E**). These phenomena were not found in HpMF-treated cells. The observed effect of 5-OH-HxMF on DNA laddering, morphological changes, chromosomal condensation, and increases in the percentage of apoptotic cells links the cytotoxic action of 5-OH-HxMF to an ability to induce apoptosis.

5-OH-HxMF-Induced Mitochondrial Apoptosis. It has been recently demonstrated that apoptosis involves the disruption of mitochondrial membrane integrity, a mechanism that is decisive for the cell death process (*10*). The effects of 5-OH-HxMF on the mitochondrial trans-membrane potential ($\Delta\Psi_m$) and the release of mitochondrial cytochrome *c* into cytosol were evaluated. A DiOC6(3) probe monitored via flow cytometry was used to measure $\Delta\Psi_m$ fluorescence.

Results of measuring fluorescence intensity in HL-60 cells exposed to 5-OH-HxMF as compared to untreated control cells are summarized in **Figure 3A**. The DiOC6(3) fluorescence intensity shifted to the left from 140.53 to 68.85, 77.44, and 70.704 in 5-OH-HxMF-induced apoptotic HL-60 cells at 15, 30, and 60 min, respectively. These results confirmed that 5-OH-HxMF causes a decrease in the mitochondrial trans-membrane potential in HL-60 cells.

The role of ROS in the induction of apoptosis is well-recognized. Results of flow cytometry analysis using DCFH-DA and DHE as fluorescent ROS, H_2O_2, and O_2 indicators demonstrate an increase in intracellular peroxide levels in 5-OH-HxMF-treated HL-60 cells. Increases of intracellular peroxide levels caused by treatment with 5-OH-HxMF were detected at 15 min and markedly increase the mean DCFH-DA fluorescence intensity from 95.52 to 119.10 and DHE fluorescence intensity from 202.96 to 251.05 (**Figure 3C**). The increase in the mean DCFH-DA fluorescence intensity suggests that an increase in ROS concentrations plays an important role as an early mediator in 5-OH-HxMF-induced apoptosis. These findings indicate that 5-OH-HxMF has an effect on mitochondrial function and the cellular accumulation of ROS. Because ROS depletes glutathione (GSH), a major antioxidant, which then allows apoptosis to proceed apoptosis, it is also likely that ROS are involved, which causes the DNA damage (*12*). A marked reduction of GSH levels was observed using the fluorescent probe CMFDA

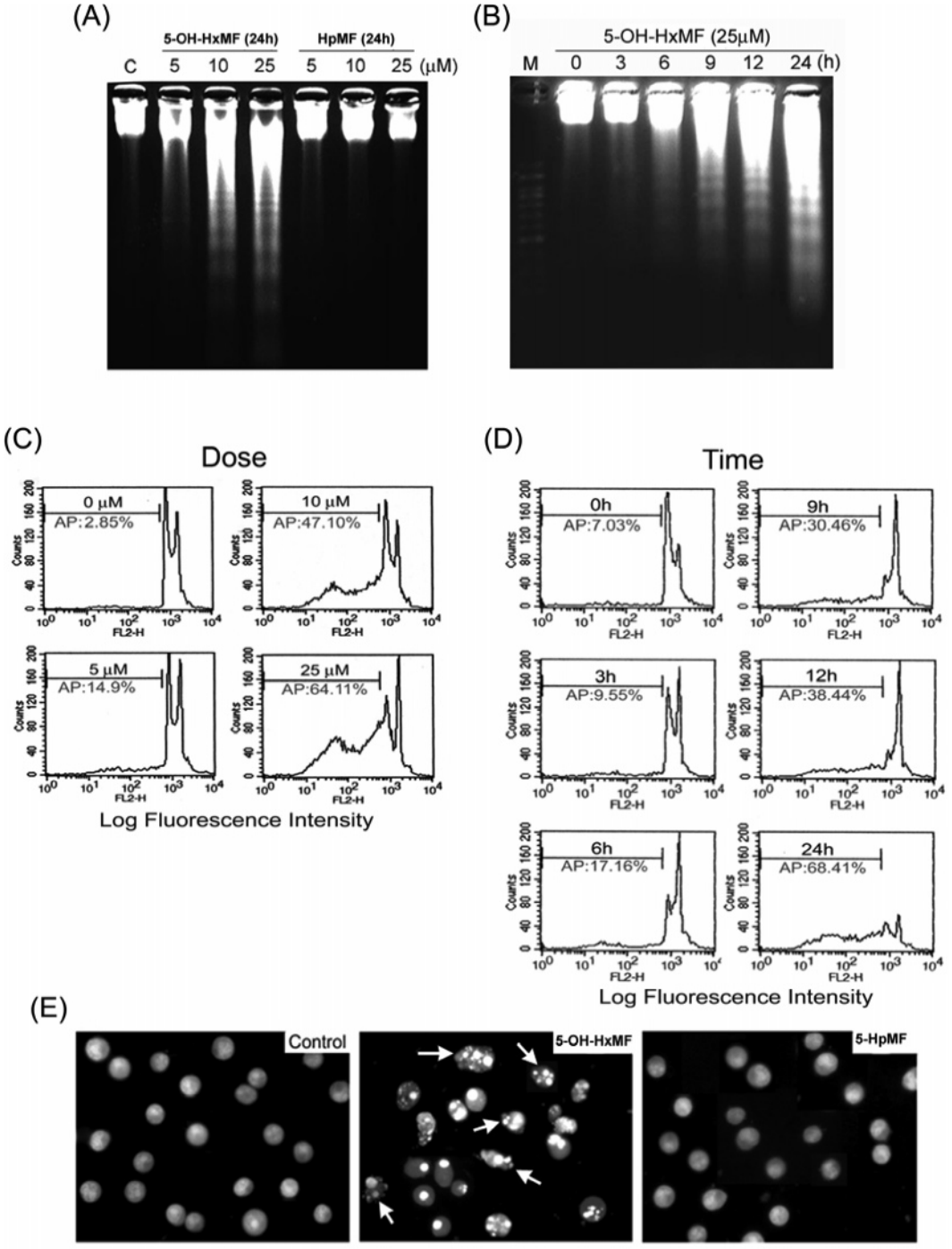

Figure 2. Induction of DNA fragmentation and chromatin condensation by 5-OH-HxMF in HL-60 cells. (**A**) HL-60 cells treated with increasing doses of 5-OH-HxMF or HpMF for 24 h or (**B**) treated with 25 μM 5-OH-HxMF for the indicated time, and internucleosomal DNA fragmentation was analyzed by agarose gel electrophoresis. M, 100 base pair DNA ladder size marker. (**C**, **D**) Determination of sub-G1 cells in 5-OH-HxMF-treated HL-60 cells by flow cytometry. The method of flow cytometry used is described in the Materials and Methods. AP (apoptotic peak) represents apoptotic cells with a lower DNA content. The data presented are representative of three independent experiments. (**E**, **C**) HL-60 cells were treated with 0.05% DMSO as vehicle control or treated with 25 μM 5-OH-HxMF for 24 h, and cells were harvested and washed with PBS followed by staining with acridine orange. The nuclear staining was examined by fluorescence microscopy. These experiments were performed at least in triplicate, and a representative experiment is presented.

(**Figure 3D**). CMFDA fluorescence intensity shifted to the left from 112.05 to 103.16 and 92.83 at 15 and 30 min, respectively. This is also indicative of the induction of apoptosis. Caspase-9 binds to Apaf-1 in a cytochrome *c* and dATP-dependent fashion to become activated and, in turn, cleaves and activates caspase-3 (*8*). As shown in **Figure 3E**, the release of mitochondrial cytochrome *c* into the cytosol was detected at 3 h in 25 μM 5-OH-HxMF-treated HL-60 cells. Further treatment of HL-60 cells with 5-OH-HxMF caused a visible increase of AIF levels in the cytoplasm, which was detectable as early as after 2 h of incubation (**Figure 3F**). Endo G is an apoptotic protein primarily residing in the intermembrane space of mitochondria. Treatment of cells for various time with 5-OH-HxMF resulted in a marked release of Endo G from the mitochondria into the cytoplasm. This was detectable after a 6 h incubation, as illustrated in **Figure 3G**. To further demonstrate whether the cytochrome *c*

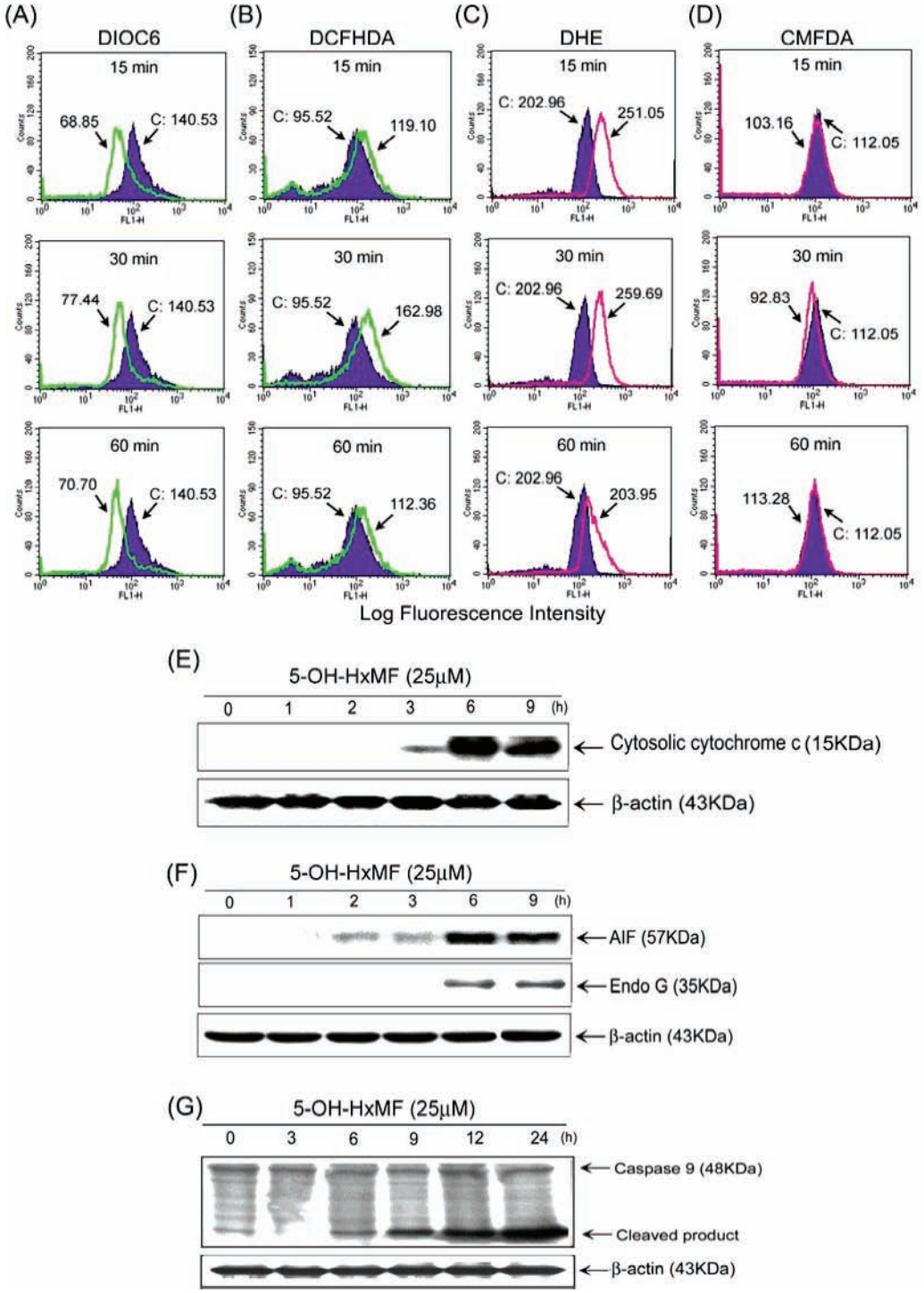

Figure 3. Induction of mitochondrial dysfunction, reactive oxygen species (ROS) generation, GSH depletion, and cytochrome *c* release following caspase-9 activation in 5-OH-HxMF-induced apoptosis. (**A**–**D**) HL-60 cells were treated with 25 μM 5-OH-HxMF for indicated times and were then incubated with 3,3′-dihexyloxacarbocyanine (40 nM), DCFH-DA (20 μM), DHE (20 μM), and CMFDA (20 μM), respectively, and analyzed by flow cytometry. Data are presented as log fluorescence intensity; C, control. (**E**–**G**) COLO 205 cells were treated with 25 μM 5-OH-HxMF for different times (1, 2, 3, 6, 9, and 12 h). Subcellular fractions were prepared as described in the Materials and Methods, and cytosolic cytochrome *c*, AIF, and Endo G were analyzed by Western blotting as described in the Material and Methods. These experiments were performed at least three times, and a representative experiment is presented.

release resulting from 5-OH-HxMF treatment would subsequently result in the cleavage and activation of pro-caspase-9, cleavage of pro-caspase-9 was sought and detected at various time points after treatment with 25 μM 5-OH-HxMF. Consistent with the timing of the cytochrome *c* release, the cleavage process of pro-caspase-9 occurred sequentially in HL-60 cells exposed in a time-dependent manner (**Figure 3H**). The sum of these observations provides clear evidence that 5-OH-HxMF-induced apoptosis operates in human leukemia HL-60 cells via a mitochondrial pathway.

5-OH-HxMF Induces Caspase Cleavage and Activation. The caspases are believed to play a central role in causing

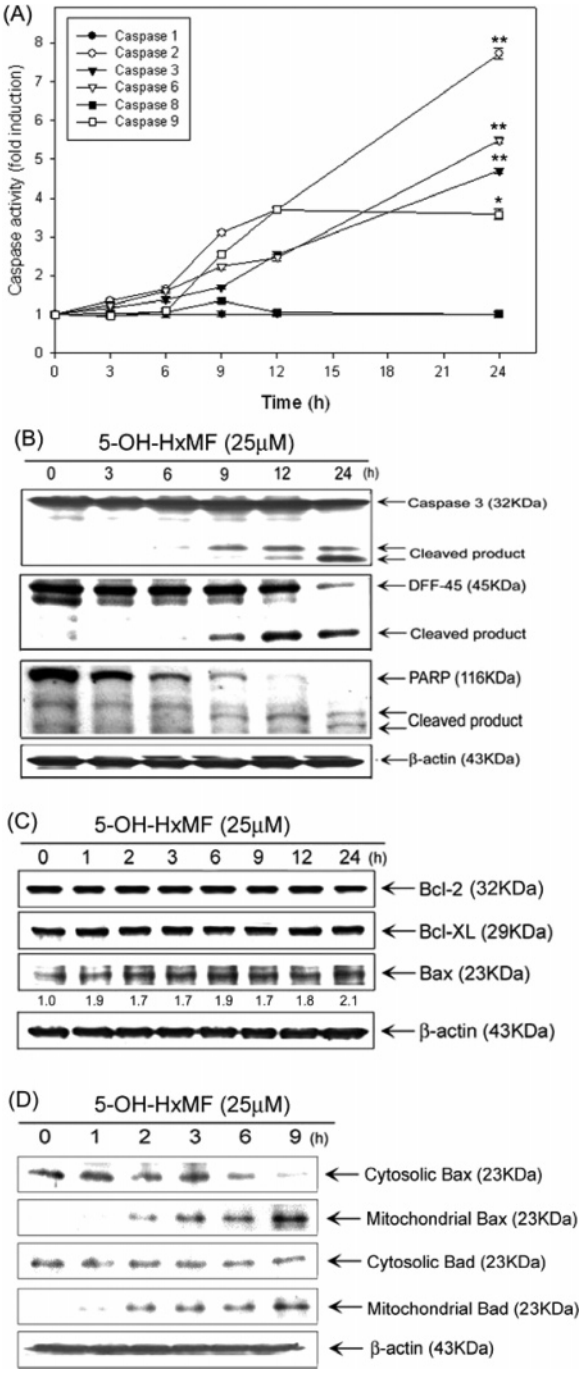

Figure 4. Induction of caspase activities, PARP cleavage, DFF-45 degradation, and Bax up-regulation during 5-OH-HxMF-induced apoptosis in HL-60 cells. (**A**) Kinetics of caspase activation in HL-60 cells. Cells were treated with 25 μM 5-OH-HxMF for different times. Caspase activities were analyzed as described in the Materials and Methods. The values are expressed as means ± SD of triplicates tests. *P < 0.05 and **P < 0.01 indicate statistically significant differences from the control group. (**B**) Western blot analyses of pro-caspase-3 in HL-60 cells were treated with 25 μM 5-OH-HxMF for different times. Degradation of pro-caspase protein represents its activation. Cleavage of PARP and DFF-45 induced by 5-OH-HxMF was time-dependent. (**C**) Western blot analyses of Bcl-2, Bcl-XL, and Bax expression in HL-60 cells that were treated for different times as described in the Materials and Methods. The values below the figure represent change in Bax protein expression of the bands normalized to β-actin. (**D**) In subcellular fractions, 5-OH-HxMF treatment led to translocation of Bax and Bad protein to the mitochondria from cytosol. These experiments were performed at least in triplicate, and a representative experiment is presented.

apoptotic responses by cleaving or degrading several cellular substrates (*20*). The enzymatic activities of caspase-1, -2, -3, -6, -8, and -9 were measured following treatment of HL-60 cells with 25 μM 5-OH-HxMF for several periods. As clearly demonstrated in **Figure 4A**, 5-OH-HxMF promoted a dramatic increase in caspase-2 activity of approximately 7.6-fold after 24 h of treatment. Additionally, caspase-3, -6, and -9 were time dependently activated by 5-OH-HxMF, but the data showed very low levels of caspase-8 and -1 activities following 5-OH-HxMF treatment. **Figure 4B** shows a gradual increase in the level of the cleavage product of caspase-3, indicating that caspase-3 was activated 9 h after 5-OH-HxMF treatment. Activation of caspase-3 causes the cleavage of PARP, a major indicator enzyme of apoptosis, to produce an 85 kDa fragment during apoptosis (*9*). As already described, ICAD is a mouse homologue of human DFF-45. Caspase-3 cleaves DFF-45, and once caspase-activated deoxyribonuclease (CAD) is released, it can enter the nucleus, where it degrades chromosomal DNA to produce interchromosomal DNA fragments (*21*, *22*). **Figure 4B** shows that the exposure of HL-60 cells to 5-OH-HxMF causes the degradation of DFF-45 protein and the degradation of 116 kDa PARP to 85 kDa fragments. The protein cleavages were associated with the activation of caspase-3. The protein expression of the Bcl-2 family was measured at different time points in 5-OH-HxMF-treated cells. A slight increase of Bax protein expression at 1 h was detected (**Figure 4C**); however, Bcl-2 and Bcl-X_L proteins remained unchanged. Immunoblot analysis of the subcellular fractions showed that 5-OH-HxMF treatment led to translocation of Bax and Bad protein to the mitochondria from the cytosol (**Figure 4D**) in a time-dependent manner. These results suggest a potential involvement of mitochondria pathway in 5-OH-HxMF-induced apoptosis in HL-60 cells.

ROS Signal Apoptosis Induced by 5-OH-HxMF. ROS have been known to be important in the induction of apoptosis. DHE and DCFH-DA were used to detect the generation of superoxides and H_2O_2/hydroxyl radicals, respectively. An increase in DCF fluorescence was observed at 15 min posttreatment with 5-OH-HxMF, and a posttreatment increase in DCFH-DA fluorescence was also seen within 15 min (**Figure 5A**,**B**). We reasoned that if ROS were a crucial factor in the induction of apoptosis, ROS scavengers must limit apoptosis. First, we tested ROS scavengers, *N*-acetylcysteine (NAC) and catalase (CAT), and observed that NAC and CAT were most efficient in limiting the increase in posttreatment DHE and DCFH-DA fluorescence, respectively (**Figure 5**). In the present study, antioxidants such as NAC, CAT, superoxide dismutase (SOD), allopurinol (ALL), pyrrolidine dithiocarbamate (PDTC), and diphenylene iodonium (DPI) were used to determine whether ROS production is an essential event for 5-OH-HxMF-induced apoptosis of HL-60 cells. As shown in **Figure 6A**, pretreatment with these antioxidants demonstrated that NAC and CAT markedly protect HL-60 cells from 5-OH-HxMF-induced apoptosis. Moreover, we also found that SOD, ALL (an xanthine oxidase inhibitor), PDTC (an NFκB inhibitor), and DPI (an NADPH oxidase inhibitor) significantly protected HL-60 cells from 5-OH-HxMF-induced apoptosis. Further experiments, using NAC and CAT, revealed a dose-dependent decrease in ROS generation (**Figure 5**) and limitation of apoptosis as assessed by PARP cleavage (**Figure 6B**). The data from these experiments demonstrate that ROS concentrations influence the result of 5-OH-HxMF-induced apoptosis and that these concentrations are controlled by the levels of available antioxidants.

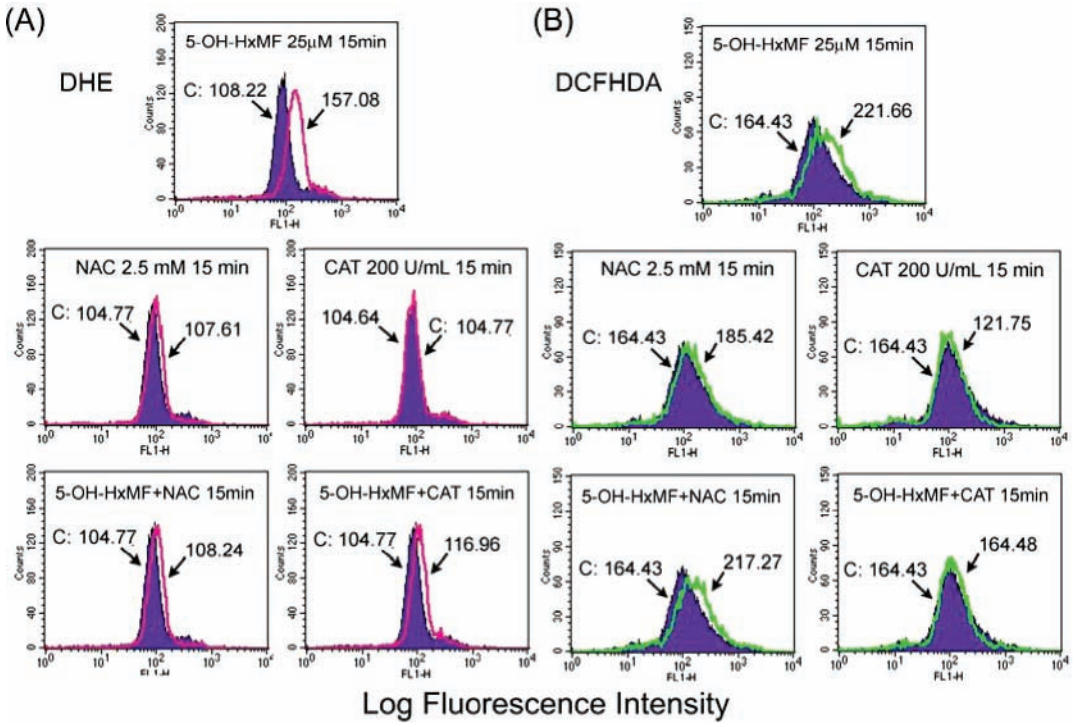

Figure 5. Effects of antioxidant, NAC, and CAT on DHE and DCFHDA fluorescence. HL-60 cells were pretreated with 2.5 mM NAC and 200 U/mL CAT for 2 h, followed by treatment with 5-OH-HxMF (25 μM), and then measured by flow cytometry. These experiments were performed at least in triplicate, and a representative experiment is presented.

Effects of Antioxidants on 5-OH-HxMF-Induced DNA Damage and GADD153 Protein Expression in HL-60 Cells. To determine if exposing HL-60 cells to 5-OH-HxMF induces DNA damage as an indicator of oxidative stress, cells were exposed to 25 μM 5-OH-HxMF for 3 h. The Comet assay was then performed to detect any single-strand breaks in the DNA (**Figure 7**). As can be seen in the representative photos from fluorescence microscopy, the nucleoids of control cells (**Figure 7A**) are uniformly spherical in shape, reflecting the absence of DNA damage. In contrast, the nucleoids of 5-OH-HxMF-treated cells appear as "comets", reflecting the presence of significant DNA damage. The typical "comet tail" illustrates that DNA single-strand breaks exist (**Figure 7B**) and is evidence of DNA damage. We speculated that the intracellular generation of ROS could be an important factor in 5-OH-HxMF-induced DNA damage. To verify this, we performed a test to determine whether antioxidants NAC and SOD could inhibit 5-OH-HxMF-induced DNA damage. As shown in **Figure 7C−F**, pretreatment with NAC significantly inhibited 5-OH-HxMF-induced DNA damage. Pretreatment with SOD demonstrated little effect. Expectedly, HpMF was not able to induce DNA damage (**Figure 7G−L**). We observed that oxidative stress promoted GADD gene activation, suggesting an involvement of ROS. To determine whether 5-OH-HxMF induced up-regulation of the GADD153 gene, Western immunoblotting analysis was performed on 5-OH-HxMF-treated cells (**Figure 7M**). As can be seen, GADD153 protein expression began to become apparent after 2 h and increased considerably in relation to the amount of time of the incubation. To determine if ROS is important in 5-OH-HxMF-induced up-regulation of GADD153 protein expression, cells were pretreated with NAC and CAT prior to exposing them to 5-OH-HxMF. NAC and CAT markedly prevented the increase in GADD153 protein expression caused by 5-OH-HxMF.

DISCUSSION

In this study, we compared the biological activity of the structurally related polymethoxylated flavones, 5-OH-HxMF and HpMF, in human cancer cells. Our results provide clear evidence that substitution of the methoxy group with a hydroxyl group in the 5-position of the flavone A ring (**Figure 1**) drastically increases biological activity of the polymethoxylated flavones. To our knowledge, this is the first demonstration that 5-OH-HxMF inhibits growth and induces apoptosis in human leukemia HL-60 cells. Among the compounds tested, 5-OH-HxMF (but not HpMF) markedly exhibited an inhibitory effect toward HL-60 cell growth (**Table 1**). HL-60 cells underwent apoptosis following treatment with 5-OH-HxMF, suggesting that apoptosis is the major cause for the growth inhibition effect of 5-OH-HxMF. Data generated from this research have clarified the molecular mechanism by which 5-OH-HxMF triggers human leukemia HL-60 cells to undergo apoptosis. As shown in **Figure 2**, 5-OH-HxMF is a strong inhibitor of cell viability and causes the potent and rapid induction of apoptosis, concurrent with DNA laddering, chromatin condensation, and apoptotic appearance in HL-60 cells. This induction of apoptosis occurrs within hours, consistent with the view that 5-OH-HxMF induces apoptosis by activating preexisting apoptotic machinery. Indeed, treatment with 5-OH-HxMF caused an induction of caspase-2, -3, -6, and -9 (but not caspase-1 and -8) associated with the degradation of DFF-45 and PARP, which preceded the onset of apoptosis (**Figure 4**).

Mitochondrial trans-membrane potential ($\Delta\Psi_m$) (often employed as an indicator of cellular viability) disruption has been implicated in a variety of apoptotic phenomena (*10*). Mitochondria have also been implicated as a source of ROS during apoptosis. Reduced mitochondrial membrane potentials have recently been shown to lead to increased generation of ROS and apoptosis (*23*). This research has demonstrated that 5-OH-HxMF disrupts the functions of mitochondria in the early stages

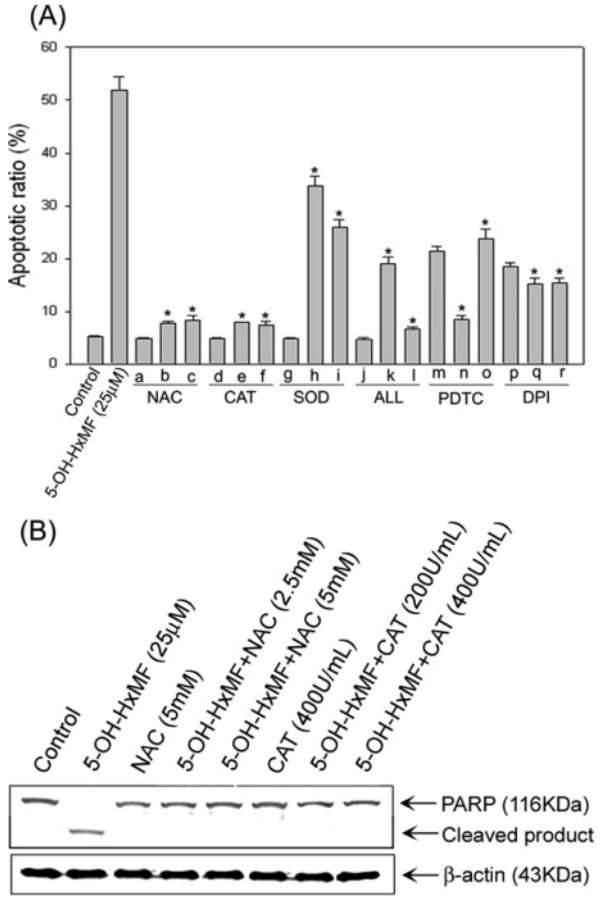

Figure 6. Effects of antioxidants on 5-OH-HxMF-treated HL-60 cells. (**A**) Effects of NAC, CAT, SOD, ALL, PDTC, and DPI on 5-OH-HxMF-treated HL-60 cells. HL-60 cells were treated with different concentrations of NAC, CAT, SOD, ALL, PDTC, and DPI for 2 h followed by 5-OH-HxMF (25 μM) treatment for another 24 h. The apoptotic ratio (%) was determined by flow cytometry. Each value is presented as the mean ± SE of three independent experiments. Key: a, NAC (5 mM); b, 5-OH-HxMF + NAC (2.5 mM); c, 5-OH-HxMF + NAC (2.5 mM); d, CAT (400 U/mL); e, 5-OH-HxMF + CAT (200 U/mL); f, 5-OH-HxMF + CAT (400 U/mL); g, SOD (200 μg/mL); h, 5-OH-HxMF + SOD (100 μg/mL); i, 5-OH-HxMF + SOD (200 μg/mL); j, ALL (100 μM); k, 5-OH-HxMF + ALL (50 μM); l, 5-OH-HxMF + ALL (100 μM); m, PDTC (40 μM); n, 5-OH-HxMF + PDTC (20 μM); o, 5-OH-HxMF + PDTC (40 μM); p, DPI (20 μM); q, 5-OH-HxMF + DPI (10 μM); and r, 5-OH-HxMF + DPI (20 μM). The asterisk denotes a statistically significant decrease as compared with values of positive control (*P < 0.05). (**B**) Effect of antioxidants on cleavage of PARP by Western blot analysis. The cells were pretreated with NAC and CAT for 2 h followed by treatment with 5-OH-HxMF for 24 h. These experiments were performed at least in triplicate, and a representative experiment is presented.

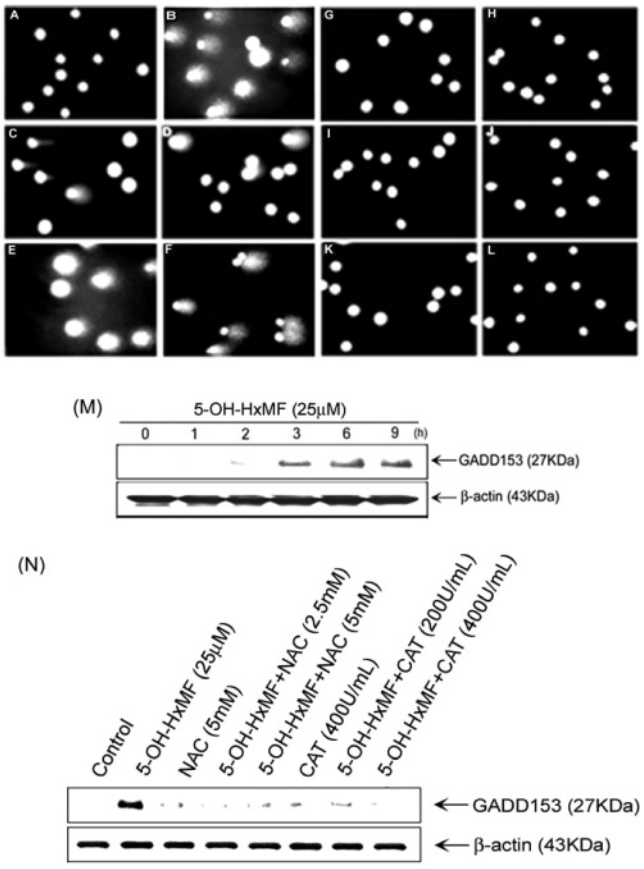

Figure 7. Effects of antioxidants on 5-OH-HxMF-induced DNA damage in HL-60 cells. (**A**) Control, (**B**) 5-OH-HxMF (25 μM), (**C**) 5-OH-HxMF + NAC (2.5 mM), (**D**) 5-OH-HxMF + NAC (5 mM), (**E**) 5-OH-HxMF + SOD (100 μg/mL), (**F**) 5-OH-HxMF + SOD (200 μg/mL), (**G**) control, (**H**) HpMF (25 μM), (**I**) HpMF + NAC (2.5 mM), (**J**) HpMF + NAC (5 mM), (**K**) HpMF + SOD (100 μg/mL), and (**L**) HpMF + SOD (200 μg/mL). (**M**) HL-60 cells were incubated with 25 μM 5-OH-HxMF for 0–9 h. Then, whole cell lysates were prepared for subsequent Western blot analysis of the GADD153 and β-actin proteins. (**N**) In testing free radical scavengers, cells were pretreated with NAC and CAT for 2 h, prior to exposure to 5-OH-HxMF for 6 h. Then, whole cell lysates were prepared for subsequent Western blot analysis of the GADD153 and β-actin proteins. These experiments were performed at least in triplicate, and a representative experiment is presented.

of apoptosis and subsequently coordinates caspase-9 activation through the release of cytochrome *c*. HL-60 cells showed increasing ROS production after 5-OH-HxMF treatment (**Figure 3**). We speculated that intracellular generation of ROS could be an important factor in 5-OH-HxMF-induced apoptosis. To verify this, we performed experiments confirming the effects of antioxidants on 5-OH-HxMF-mediated apoptosis. Pretreatment with the antioxidants, NAC, CAT, SOD, ALL, PDTC, and DPI (used as free radical scavengers) caused a significant inhibition in 5-OH-HxMF-induced apoptosis (**Figure 6**). As a significant novel finding in the present study, 5-OH-HxMF increased expression of the GADD153 gene, which has been acknowledged as a proapoptosis gene (*24*). Because the GADD153 gene is typically induced in response to cellular DNA damage and ER stress, it is suggested that 5-OH-HxMF-induced up-regulation of GADD153 mRNA could be an early transcriptional response to 5-OH-HxMF (**Figure 7**). Furthermore, increased GADD153 expression was essentially prevented by CAT and NAC, which are known to markedly increase the intracellular concentration of reduced glutathione (*25*), suggesting that a redox mechanism was involved in promoting GADD153 mRNA expression. The intracellular GSH:GSSG ratio is known to influence the expression of redox sensitive genes (*26*). Although the full significance of up-regulation of GADD153 gene expression in 5-OH-HxMF-treated HL-60 cells is not known, the effect of 5-OH-HxMF on GADD153, in particular, might contribute to the capacity of 5-OH-HxMF-induced apoptosis. Thus, the sum of these results suggests that the GADD153 gene may be an important target gene for apoptotic cell death induced by 5-OH-HxMF. These findings suggest that GADD153 expression may modulate the sensitivity of HL-60 cells to apoptosis triggered by 5-OH-HxMF-induced DNA damage (**Figure 7**). Moreover, NAC inhibited 5-OH-HxMF-induced DNA damage and apoptosis. Further studies will

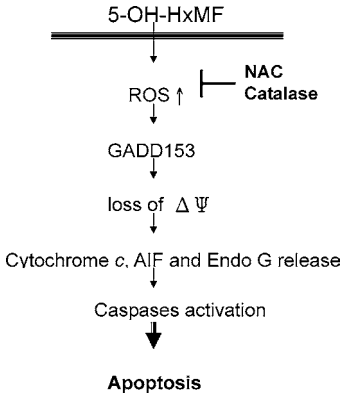

Figure 8. Schematic representation of mechanisms of action of 5-OH-HxMF-induced apoptosis in HL-60 cells. The initial event induced by 5-OH-HxMF induction of ROS production and the coordinated modulation GADD153 gene expression would promote mitochondrial dysfunction (loss of mitochondrial membrane potential), resulting in cytochrome *c*, AIF, and Endo G release, caspases activation, and apoptotic death.

be required to elucidate how 5-OH-HxMF modulates expression of the GADD153 protein. We do not rule out the possible mechanism that 5-OH-HxMF could directly penetrate into cells via the cell membrane, directly target the ER, leading to an increase in ER stress. The Bcl-2 family of proteins, whose members may be antiapoptotic or proapoptotic, regulate cell death by controlling mitochondrial membrane permeability during apoptosis (*27*). We therefore inferred that the Bcl-2 family proteins may participate in the seminal event that controls the change in mitochondrial membrane potential, triggering cytochrome *c* release during apoptosis induced by 5-OH-HxMF. In our study, we found up-regulation of Bax expression during 5-OH-HxMF-induced apoptosis in HL-60 cells (**Figure 4**). Consistent with a model in which the ratio of antiapoptotic to proapoptotic proteins determines cellular susceptibility to apoptosis (*28*), the lower ratio of Bcl-2 to Bax was inversely correlated to the increase of incubation times after 5-OH-HxMF treatment.

Although 5-OH-HxMF can change the integrity of the mitochondrial membrane by regulating the expression of Bcl-2 family proteins, again, we do not rule out a possible mechanism in which 5-OH-HxMF penetrates cells and directly targets mitochondria, thereby increasing membrane permeability with an attendant decrease of $\Delta\Psi_m$, accompanied by ROS production. On the basis of this data, we propose an apoptotic mechanism caused by 5-OH-HxMF. The initial event induced by 5-OH-HxMF is likely an induction of ROS, primarily based on the observation that NAC and CAT prevent apoptosis.

Taken collectively, the current findings can be interpreted to propose a temporal sequence of events related to the effects of 5-OH-HxMF on HL-60 cells (**Figure 8**). Analyses of expression of Bcl-2 family proteins, generation of ROS, the subcellular locations of cytochrome *c*, AIF, Endo G, Bax, and Bad, and the status of various caspase activities suggest that apoptosis induced by 5-OH-HxMF in HL-60 cells was primarily associated with promotion of ROS production, DNA damage, and mitochondrial dysfunction. The initial event induced by 5-OH-HxMF likely causes increased induction of ROS production and coordinative modulation of GADD153 gene expression. This is followed by GADD153 protein promotion of mitochondrial dysfunction (loss of mitochondrial membrane potential), resulting in cytochrome *c* release, caspase activation, and apoptotic death. Further studies are needed to determine whether DNA damage and the GADD153 protein directly initiate apoptosis in HL-60 cells exposed to 5-OH-HxMF. In summary, we have provided the basis for a molecular mechanism for apoptosis mediated by 5-OH-HxMF as a potential cancer treatment. The potential application of 5-OH-HxMF in the inhibition of cancer cell proliferation would make it an attractive agent for human leukemia research and, possibly, treatment.

ABBREVIATIONS USED

5-OH-HxMF, 5-hydroxy-3,6,7,8,3′,4′-hexamethoxyflavone; HpMF, 3,5,6,7,8,3′,4′-heptamethoxyflavone; DFF, DNA fragmentation factor; PARP, poly(ADP-ribose)polymerase; GADD153, growth arrest and DNA damage-inducible gene 153; NAC, *N*-acetylcysteine; GSH, glutathione; ALL, allopurinol; CAT, catalase; DCFH-DA, dichlorodihydrofluorescein diacetate; PDTC, pyrrolidine dithiocarbamate; DPI, diphenylene iodonium; ROS, reactive oxygen species; SOD, superoxide dismutase.

LITERATURE CITED

(1) Pan, M. H.; Chen, W. J.; Lin-Shiau, S. Y.; Ho, C. T.; Lin, J. K. Tangeretin induces cell-cycle G1 arrest through inhibiting cyclin-dependent kinases 2 and 4 activities as well as elevating Cdk inhibitors p21 and p27 in human colorectal carcinoma cells. *Carcinogenesis* **2002**, *23* (10), 1677−1684.

(2) Bas, E.; Recio, M. C.; Giner, R. M.; Manez, S.; Cerda-Nicolas, M.; Rios, J. L. Anti-inflammatory activity of 5-O-demethylnobiletin, a polymethoxyflavone isolated from Sideritis tragoriganum. *Planta Med.* **2006**, *72* (2), 136−142.

(3) Li, S.; Lo, C. Y.; Ho, C. T. Hydroxylated polymethoxyflavones and methylated flavonoids in sweet orange (*Citrus sinensis*) peel. *J. Agric. Food Chem.* **2006**, *54* (12), 4176−4185.

(4) Li, S.; Wang, Z.; Sang, S.; Huang, M. T.; Ho, C. T. Identification of nobiletin metabolites in mouse urine. *Mol. Nutr. Food Res.* **2006**, *50* (3), 291−299.

(5) Murakami, A.; Nakamura, Y.; Torikai, K.; Tanaka, T.; Koshiba, T.; Koshimizu, K.; Kuwahara, S.; Takahashi, Y.; Ogawa, K.; Yano, M.; Tokuda, H.; Nishino, H.; Mimaki, Y.; Sashida, Y.; Kitanaka, S.; Ohigashi, H. Inhibitory effect of citrus nobiletin on phorbol ester-induced skin inflammation, oxidative stress, and tumor promotion in mice. *Cancer Res.* **2000**, *60* (18), 5059−5066.

(6) Hong, W. K; Sporn, M. B. Recent advances in chemoprevention of cancer. *Science* **1997**, *278* (5340), 1073−1077.

(7) Sporn, M. B.; Suh, N. Chemoprevention of cancer. *Carcinogenesis* **2000**, *21* (3), 525−530.

(8) Martin, S. J.; Green, D. R. Protease activation during apoptosis: Death by a thousand cuts? *Cell* **1995**, *82* (3), 349−352.

(9) Earnshaw, W. C.; Martins, L. M.; Kaufmann, S. H. Mammalian caspases: Structure, activation, substrates, and functions during apoptosis. *Annu. Rev. Biochem.* **1999**, *68*, 383−424.

(10) Li, P.; Nijhawan, D.; Wang, X. Mitochondrial activation of apoptosis. *Cell.* **2004**, *116* (2 Suppl.), S57−S59, 2.

(11) Rao, R. V.; Ellerby, H. M.; Bredesen, D. E. Coupling endoplasmic reticulum stress to the cell death program. *Cell Death Differ.* **2004**, *11* (4), 372−380.

(12) Ikeyama, S.; Wang, X. T.; Li, J.; Podlutsky, A.; Martindale, J. L.; Kokkonen, G.; van, H. R.; Gorospe, M.; Holbrook, N. J. Expression of the pro-apoptotic gene gadd153/chop is elevated in liver with aging and sensitizes cells to oxidant injury. *J. Biol. Chem.* **2003**, *278* (19), 16726−16731.

(13) Maytin, E. V.; Ubeda, M.; Lin, J. C.; Habener, J. F. Stress-inducible transcription factor CHOP/gadd153 induces apoptosis in mammalian cells via p38 kinase-dependent and -independent mechanisms. *Exp. Cell Res.* **2001**, *267* (2), 193−204.

(14) Tombal, B.; Weeraratna, A. T.; Denmeade, S. R.; Isaacs, J. T. Thapsigargin induces a calmodulin/calcineurin-dependent apoptotic cascade responsible for the death of prostatic cancer cells. *Prostate* **2000**, *43* (4), 303−317.

(15) Yang, J.; Liu, X.; Bhalla, K.; Kim, C. N.; Ibrado, A. M.; Cai, J.; Peng, T. I.; Jones, D. P.; Wang, X. Prevention of apoptosis by Bcl-2: Release of cytochrome c from mitochondria blocked. *Science* **1997**, *275* (5303), 1129−1132.
(16) Pan, M. H.; Chang, W. L.; Lin-Shiau, S. Y.; Ho, C. T.; Lin, J. K. Induction of apoptosis by garcinol and curcumin through cytochrome c release and activation of caspases in human leukemia HL-60 cells. *J. Agric. Food Chem.* **2001**, *49* (3), 1464−1474.
(17) Pan, M. H.; Lin, J. H.; Lin-Shiau, S. Y.; Lin, J. K. Induction of apoptosis by penta-O-galloyl-beta-D-glucose through activation of caspase-3 in human leukemia HL-60 cells. *Eur. J. Pharmacol.* **1999**, *381* (2−3), 171−183.
(18) Pan, M. H.; Sin, Y. H.; Lai, C. S.; Wang, Y. J.; Lin, J. K.; Wang, M.; Ho, C. T. Induction of apoptosis by 1-(2-hydroxy-5-methylphenyl)-3-phenyl-1,3-propanedione through reactive oxygen species production, GADD153 expression, and caspases activation in human epidermoid carcinoma cells *J. Agric. Food Chem.* **2005**, *53* (23), 9039−9049.
(19) Hanahan, D.; Weinberg, R. A. The hallmarks of cancer. *Cell* **2000**, *100* (1), 57−70.
(20) Li, P.; Nijhawan, D.; Budihardjo, I.; Srinivasula, S. M.; Ahmad, M.; Alnemri, E. S.; Wang, X. Cytochrome c and dATP-dependent formation of Apaf-1/caspase-9 complex initiates an apoptotic protease cascade. *Cell* **1997**, *91* (4), 479−489.
(21) Liu, X.; Zou, H.; Slaughter, C.; Wang, X. DFF, a heterodimeric protein that functions downstream of caspase-3 to trigger DNA fragmentation during apoptosis. *Cell* **1997**, *89* (2), 175−184.
(22) Sakahira, H.; Enari, M.; Nagata, S. Cleavage of CAD inhibitor in CAD activation and DNA degradation during apoptosis. *Nature* **1998**, *391* (6662), 96−99.
(23) Marchetti, P.; Castedo, M.; Susin, S. A.; Zamzami, N.; Hirsch, T.; Macho, A.; Haeffner, A.; Hirsch, F.; Geuskens, M.; Kroemer, G. Mitochondrial permeability transition is a central coordinating event of apoptosis. *J. Exp. Med.* **1996**, *184* (3), 1155−1160.
(24) Xia, Y.; Wong, N. S.; Fong, W. F.; Tideman, H. Upregulation of GADD153 expression in the apoptotic signaling of N-(4-hydroxyphenyl)retinamide (4HPR). *Int. J. Cancer* **2002**, *102* (1), 7−14.
(25) Meister, A. Glutathione deficiency produced by inhibition of its synthesis, and its reversal; applications in research and therapy. *Pharmacol. Ther.* **1991**, *51* (2), 155−194.
(26) Arrigo, A. P. Gene expression and the thiol redox state. *Free Radical Biol. Med.* **1999**, *27* (9−10), 936−944.
(27) Adams, J. M.; Cory, S. The Bcl-2 protein family: Arbiters of cell survival. *Science* **1998**, *281* (5381), 1322−1326.
(28) Tsujimoto, Y. Role of Bcl-2 family proteins in apoptosis: Apoptosomes or mitochondria? *Genes Cells* **1998**, *3* (11), 697−707.

Received for review January 10, 2007. Revised manuscript received April 22, 2007. Accepted April 26, 2007. This study was supported by the National Science Council NSC 95-2321-B-022-001 and NSC 95-2313-B-022-003-MY3.

JF070068Z